

# Recent developments in quantum key distribution: theory and practice

Wolfgang Mauerer\*, Wolfram Helwig, and Christine Silberhorn

Max Planck Research Group, Institute of Optics, Information and Photonics, Integrated Quantum Optics Group, University of Erlangen-Nürnberg, Günther-Scharowsky-Straße 1/Bau 24, 91058 Erlangen, Germany

Received 30 November 2007

**Key words** Quantum cryptography, quantum communication, experimental imperfections.

**PACS** 03.67.Dd, 03.67.Hk

*In honour of Max Planck (1858–1947) on the occasion of his 150th birthday.*

Quantum key distribution is among the foremost applications of quantum mechanics, both in terms of fundamental physics and as a technology on the brink of commercial deployment. Starting from principal schemes and initial proofs of unconditional security for perfect systems, much effort has gone into providing secure schemes which can cope with numerous experimental imperfections unavoidable in real world implementations. In this paper, we provide a comparison of various schemes and protocols. We analyse their efficiency and performance when implemented with imperfect physical components. We consider how experimental faults are accounted for using effective parameters. We compare various recent protocols and provide guidelines as to which components propose best advances when being improved.

## 1 Introduction

During the last decade, quantum key distribution (QKD) was established among the most active and productive research fields in quantum physics. Sharing secret information between remote parties is not only a practical problem, but has interesting outreach into numerous fields ranging from information theory to fundamental physics. Although the fundamental ideas of QKD were already laid out around 1970 by Stephen Wiesner, they were not published until a decade later, in 1983 [1]. The year 1984 brought the seminal proposal of Charles Bennett and Gilles Brassard in form of the BB84 key distribution protocol [2]. It was followed by numerous alternative variants and improvements (e.g., [3–6]), but the methods usually remain closely related to the original proposal.

The basic idea of QKD is as follows. Two parties, which we name Planck and Bohr (it is also common to refer to them as Alice and Bob), establish a shared secret key between them because they want to discuss sensible facts about their theories. The malicious eavesdropper Einstein (alternatively called Eve in a cryptographic context) who possesses unlimited technological power – only restricted by the laws of quantum mechanics – does not believe in Planck’s and Bohr’s theory. He would like to listen to their communication in order to prove their arguments wrong. Fortunately, their quantum theory is right, and he is not able to gain any information about the shared secret key. This key is used to encode information, and the encoding can be shown to be perfectly secure provided the key is only known to Planck and Bohr. Thus quantum cryptography is referred to as unconditionally secure.

Security proofs for QKD schemes are solely based on the laws of physics and do not use any assumptions about computational complexity – in contrast to purely classical schemes. Real world effects like lossy transmission or imperfect detectors are unavoidable in practice. Nevertheless, security can also be proved under these circumstances. The obtainable key rates and achievable transmission distance highly depend on the utilised hardware. It is important to select components such that optimal performance is

---

\* Corresponding author E-mail: wolfgang.mauerer@ioip.mpg.de

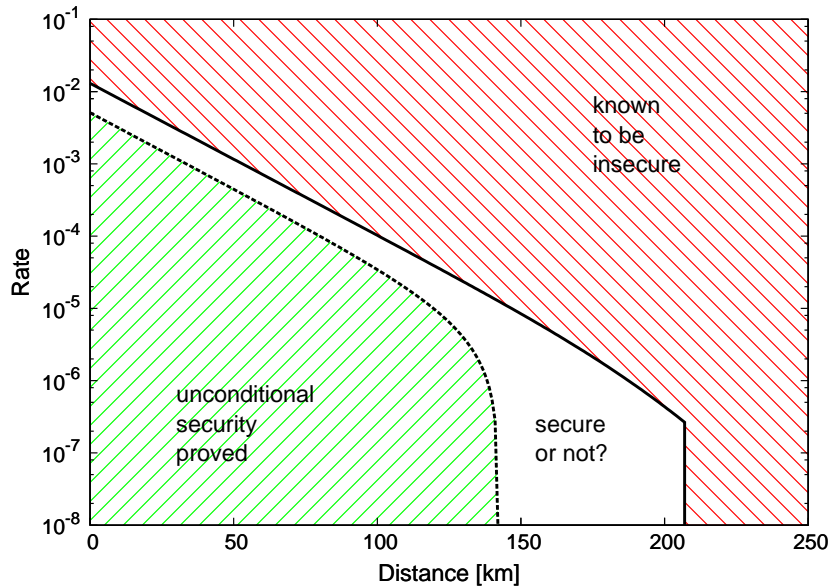


**Fig. 1** Typical performance diagram for a QKD system. The dashed line represents a lower bound on the secret key rate. This means it can be proven that at a given distance, *at least* this number of secret bits can be transmitted per pulse. The solid line provides fundamental physical upper bounds, and it is known that no secret key can be established beyond this distance respectively that no larger number of secret bits per transmitted pulse can be obtained. The region between the lower and upper bound is unknown terrain: It is still undecided if secure QKD is possible in this area. The aim of current research is therefore to increase the lower bounds (e.g., [6, 9–11]) and decrease the upper bounds (e.g., [10, 12, 13]). Section 3.3.2 introduces one scheme which nearly closes this gap. The key rate is given in secret bits per pulse, and must be multiplied with the repetition rate of the source to obtain the proper data rate. With current technology, the maximal repetition rate is not limited by the source, but mainly by the dead time of detectors, cf. Ref. [14].

achieved. In this paper, we will present a survey of a number of available protocols. We will also discuss how imperfections affect their performance, and how to choose the best hardware. This includes advice on which components need to be optimised in various practical settings to obtain best results.

General reviews about QKD can be found in References [7, 8], and we will therefore not try to provide a detailed elementary introduction in this paper, but refer the reader to the mentioned references to become acquainted with the basic concepts. The principal setting of every QKD protocol between two parties is depicted in Fig. 2. The performance of QKD systems is usually visualised in terms of diagrams which plot the secret key rate over transmission distance. Fig. 1 shows an example, and the reader is referred to the caption for information on how to interpret such a diagram.

## 2 QKD hardware

We now turn our attention to the hardware used for signal generation, transmission and reception. Security proofs require idealised components. Unavoidable experimental imperfections are handled by introducing effective error parameters, and we will concentrate on these in the following.<sup>1</sup> Note that Table 1 provides a hardware comparison for recently performed QKD experiments.

Before we commence further, we would like to point to “equation” (77) from Ref. [8]:

$$\text{Infinite security} \Rightarrow \text{Infinite cost} \Rightarrow \text{Zero practical interest.} \quad (1)$$

<sup>1</sup> Obviously imperfect components must be described by a physical model. Additional attacks can become feasible – possibly even classical attacks – if side effects arise which are not included in the model.

This means that practical usability is required for every QKD system – cryptography is no good if everyone sends everything unencrypted because no one can afford to use encryption. Therefore, it is especially important to consider real-world applicability. This means especially cost and technological feasibility. While there may often be better (research) alternatives for a given component, we concentrate on the solutions which are not only available in quantities, but also come at a reasonable price.

## 2.1 Photon sources

Transmitting quantum signals requires a signal source. With few exceptions, the protocols considered in this paper deally require single photons. This can be achieved in practice, but only at a great expense and experimental effort, see, for instance, Ref. [15]. In current practice, two sources for QKD are conventionally employed: attenuated lasers and parametric downconversion (PDC) sources.

### 2.1.1 Attenuated laser beams

The quantum state emitted by a laser is a coherent state which can be uniquely characterised by a complex value  $\alpha$ . A representation in the Fock basis is given by

$$|\psi\rangle = e^{-\frac{|\alpha|^2}{2}} \sum_{n=0}^{\infty} \frac{\alpha^n}{\sqrt{n!}} |n\rangle. \quad (2)$$

Under the assumption that no phase reference for the state exists once it has left Planck’s control [8], we can write  $\alpha = \mu e^{i\theta}$  for  $\mu, \theta \in \mathbb{R}$ , and the corresponding phase averaged density operator becomes

$$\hat{\rho} = \frac{1}{2\pi} \int d\theta |\mu e^{i\theta}\rangle \langle \mu e^{i\theta}| = \sum_n p(n) |n\rangle \langle n|. \quad (3)$$

The probability distribution  $p(n)$  is given by

$$p(n) = e^{-|\alpha|^2} \frac{|\alpha|^{2n}}{n!}, \quad (4)$$

i.e., a Poissonian distribution, and the density operator represents a classical mixture of photon number states.

To approximate the desired single-photon source, the intensity (i.e.,  $\mu$ ) is chosen such that the probability of emitting a two-photon Fock state is low. Unfortunately, with less intensity, vacuum contributions (i.e., Fock states with zero photons) become more and more frequent. In a laser pulse based system, it is therefore essential to optimise the intensity such that key rate and transmission distance are maximised.

### 2.1.2 Parametric downconversion

In a PDC process [16], an optical medium with nonlinear susceptibility  $\chi^{(2)}$  is pumped by a laser to generate photon-number entangled states of the form  $|\psi\rangle \propto \sum_{n=0}^{\infty} c_n |n\rangle_S |n\rangle_I$ . The subscripts S and I refer to two spatial modes which are conventionally denoted by “signal” and “idler”. If the spectrum of the state is approximately a single frequency mode, the distribution  $p(n)$  is thermal, i.e.,  $c_n = \lambda^n$ . Current results however indicate that the photon number distribution will shift to a Poissonian distribution the more frequencies contribute to the state, cf. Ref. [17, 18]. Irregardless of the statistical distribution, PDC sources provide two distinct advantages in comparison to lasers.

- The second spatial mode can be used as a trigger, resulting in a heralded photon source [19–21]. This enables to filter out vacuum contributions, resulting in considerably increased maximal secure distance [22–24].

- In combination with the decoy method (refer to Section 3.3), several techniques have been devised to gain higher transmission rates and distances [24, 25].
- Entanglement-based protocols as introduced by Ekert in 1991 [4] become possible.

Note that the advantage of parametric downconversion comes only into play if a satisfactory source efficiency can be achieved. This has not been the case for crystal-based sources which used to be state of the art a couple of years ago [26]. The technique of waveguided parametric downconversion [27–30] and photon pair generation by four-wave mixing in dispersion-shifted and photonic crystal fibres [31, 32] could provide many improvements in the future. By now, the brightness of PDC is larger than required, cf. [21, 33].

## 2.2 Detectors

The detection process poses two requirements. Firstly, different orthogonal signals need to be distinguished. Secondly, the detector needs to announce if a signal arrived or not.

The decoding of orthogonally polarised signals depends on the particular protocol, but can always be achieved by a polarising beam splitter or an interferometer. Experimental imperfections can, for instance, arise from a geometric misalignment of components. With a certain probability, Bohr receives a logical “zero”, but detects a “one” instead, and vice versa. The error is conventionally referred to as *misalignment*, and the probability with which such an error occurs is denoted by  $e_{\text{det}}$ . Note, that errors which occur in the preparation stage can, as well as transmission errors, be subsumed into detection misalignment.

The detection problem is usually more involved. Although Planck might have sent off a pulse, losses during the transmission can have led to complete extinction, especially at longer distances. Owing to dark counts, a detector can nevertheless click although no signal is present. The probability for this to happen is denoted by  $p_{\text{dark}}$ . With current technology, it is hard to reliably detect single quanta of light because of non-unit quantum detection efficiency. A number of possibilities are available. Most commonly avalanche photo diodes (APDs) are employed, but there are alternatives, e.g., quantum dot detectors, visible light photocounters, superconducting detectors etc. [7]. All suffer from quantum efficiencies much below one. In the following, we will denote the probability to detect an incoming single photon with  $\eta_{\text{det}}$ . The typical value depends highly on the wavelength used. While devices operating at 800 nm provide efficiencies of up to 80%, the typical level for telecommunication wavelengths ( $\approx 1550$  nm) is only around 5%.

Click detectors with 100% quantum efficiency would allow to distinguish between different orthogonal polarisations using a single detector: A click represents one specific polarisation, and no click ensures that the orthogonal polarisation was present. Under the influence of loss, this will not work anymore: When a “no click” event takes place, it is impossible to distinguish between the second polarisation mode and a lost signal. Therefore all practical QKD systems use two detectors to analyse the basis of the transmitted signal.

## 2.3 Information encoding

Albeit arbitrary quantum systems can be used to encode information on them, the use of light is a natural choice for present-day systems. Since binary systems are the canonical fundamental of information science, the two-level property is also carried into the quantum domain – and called qbit accordingly. Two orthogonal states are required to encode one classical bit with values 0 and 1. The polarisation of a photon (which is equivalent to a spin  $\frac{1}{2}$ -system) provides two orthogonal states, for instance horizontal  $|\leftrightarrow\rangle$  and vertical  $|\updownarrow\rangle$  polarisation. It is possible to form arbitrary superpositions of these states. Physically, the preparation of polarised light is a standard task easily achieved by wave plates. On the detection side, a polarising beam splitter is sufficient to distinguish between orthogonal polarisations.

Transmitting four differently polarised photons across fibres is challenging: Polarisation mode dispersion leads to polarisation rotation. Although there are polarisation maintaining fibres which preserve a single polarisation mode well, these cannot be used for QKD because states with different, non-orthogonal

polarisations need to be transmitted. Fibre-based polarisation coding can in general only be employed at short distances.

To remedy this drawback, an equivalent of a two-level system which is not based on polarisation needs to be employed. Phase encoding [8] is mathematically equivalent to a two-level system, and thus to photon polarisation. By providing a phase reference to Bohr, Planck can prepare signals with a defined phase, and Bohr can detect this phase using an interferometric setup. Certain phase differences are assigned to one bit value, and others to the conjugate value. One particular problem arising here is phase mismatch of the interferometer, but this problem can be controlled with current technology.

#### 2.4 Transmission

There are basically two alternatives to transmit light from Planck to Bohr: Over fibres, and across free space. It highly depends on the wavelength which method is more favourable to deploy. For the telecommunication wavelengths around 1550 nm, much research and engineering effort has gone into optimising fibre transmission. Current damping rates are at 0.21 dB/km. This is quite close to the technological limits [8]<sup>2</sup>, and huge improvements are not to be expected.

The second wavelength region commonly employed is 800 nm, but fibres in this region display large damping. Free space transmission is therefore the most reasonable option. However, signal transmission only works when a sight contact can be established, and weather conditions have a significant impact on the attenuation. On a clear, calm night at best weather conditions, the damping can be comparable to fibre transmission at 1550 nm, but storm, clouds and mist can make damping rise to levels of over 20 dB/km [7]. It is crucial to observe that the detection benefits at 800 nm are compensated by the disadvantages of transmission, and vice versa for 1550 nm.

### 3 Quantum key distribution protocols

A two-stage strategy is employed to establish a secret key between Planck and Bohr which can be used to encrypt messages with perfect security.

- In the first stage, Planck transmits quantum mechanical signals to Bohr via a quantum channel. Since the signals obey the laws of quantum mechanics (especially the no-cloning theorem [34]), measurements by Einstein will inevitably modify the state. These modifications manifest themselves as noise on the receiver side. If the noise exceeds a certain threshold, Einstein has potentially gained too much information about the signal, and the honest parties abort the protocol. Usually, the first stage of a QKD protocol is called *quantum stage*.
- The key shared between Planck and Bohr still contains errors, and Einstein may possess partial knowledge. Classical methods (error correction (EC) and privacy amplification (PA), see [7, 8]) are used in the second stage to remedy these. This stage can also include a sifting step, cf. Section 3.1, in which inconclusive measurement results are removed. Conventionally, the second stage is called *classical stage* of a QKD protocol.

Once a perfect secret key between Planck and Bohr is established, a classical method can be employed to perform the actual encryption: the one-time pad, also called Vernam cipher. This method has been known for a very long time [35], and provides perfect, unbreakable security irregardless of any technological constraints. The bits of a message  $m$  are added (naturally modulo 2) to the bits of the secret key  $k$ , generating the cipher text  $c = k \oplus m$ . The encrypted message  $c$  is then sent to Bohr, and the plain text can be recovered if and only if the key  $k$  is known:  $m = c \oplus k$ .

---

<sup>2</sup> In principle, loss-less transmission would be possible by using teleportation. For this reason, we must assume that Einstein has quantum channels capable of transmitting signals without *any* loss, since no fundamental physical reason prevents the existence of such channels.

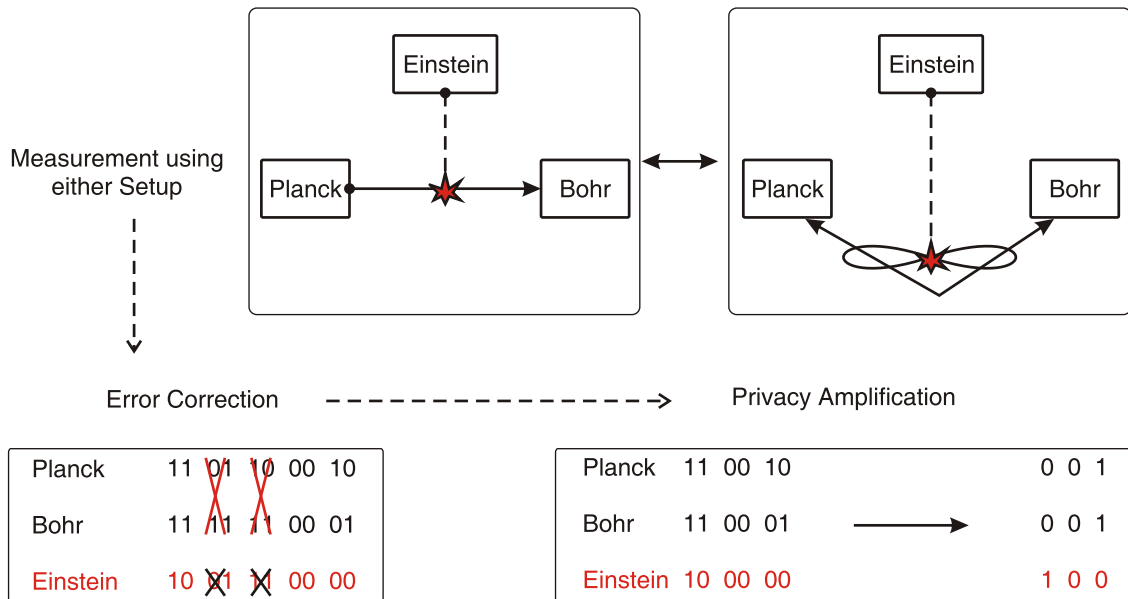


**Fig. 2** General structure of quantum key distribution. Planck provides a number of quantum mechanical signals to Bohr, and the eavesdropper Einstein tries to listen undetected. Employing various techniques described in this paper, Planck and Bohr can, however, generate a string of secret bits about which Einstein has no information whatsoever. Starting from this key, classical mathematical methods can be employed to communicate in perfect security.

In this paper, we restrict our attention to discrete variable protocols.<sup>3</sup> They use single quanta (or a very low number of quanta) of the electromagnetic field which are most conveniently described in a Fock space. Spin  $\frac{1}{2}$ -like properties are usually used to encode and transmit information. Obviously, this approach requires dark light beams with very low intensities and provides corresponding experimental challenges, but is well suited for security proofs. Discrete variable protocols come in two flavours.

- In a *prepare and measure* (p&m) protocol, Planck prepares a quantum state and sends it to Bohr, who performs a measurement. A random choice of non-orthogonal encoding and measurement bases (see Section 3.1) guarantees that Einstein cannot obtain perfect information about the transmitted states.
- On the other hand, in an *entanglement based* scheme, entangled photon pairs are utilised for key generation. One photon is given to Planck, and another to Bohr. Note, that the source of entangled states need not be located with the honest parties, and can even be placed under Einstein's control [37]! Planck and Bohr must ensure that they share a maximally entangled state. This can, for instance, be generated from a number of noisy non-maximally entangled states via entanglement purification and distillation [8] (however, the physical operations required can effectively be replaced by EC and PA). Measurements on both sides will result in perfect correlations and Einstein cannot infer information at all.

It is interesting to observe that security proofs for p&m schemes are often founded on an entanglement based protocol operating on maximally entangled states, followed by stepwise reduction to the p&m situation, cf. [38]. Experimental implementation differs in quite many details though. We consider both, prepare and measure schemes as well as entanglement based key distribution.

Classical communication between Planck and Bohr is necessary to perform various tasks required for QKD. This communication is made publically available such that Einstein cannot modify it once it has

<sup>3</sup> Continuous variable protocols where key distribution is achieved by employing conjugate quadratures for bright beams are an alternative. We refer the reader to the Review [36] for more information.

been sent off. Nevertheless, it remains a problem to ensure that the origin of communication is really the intended person. This can be solved classically by using *authenticated channels*. Since implementing an authenticated channel requires a shared secret key, a causality dilemma arises: How can the key required for authentication be transmitted? A short initial secret key shared between Planck and Bohr is required. Because of this dependency, QKD is thus referred to more exactly as *quantum key growing*.

### 3.1 BB84

BB84 is a p&m scheme which relies on two sets of orthogonal bases, provided by any two-level quantum system, for instance photon polarisation, phase encoding, or even Spin  $\frac{1}{2}$  systems [7, 8]. Set 1 consists of the two states  $|\uparrow\rangle$  and  $|\leftrightarrow\rangle$  with  $\langle\uparrow|\leftrightarrow\rangle = 0$ . Set 2 contains the states  $|+\rangle \equiv \frac{1}{\sqrt{2}}(|\uparrow\rangle + |\leftrightarrow\rangle)$  and  $|-\rangle \equiv \frac{1}{\sqrt{2}}(|\uparrow\rangle - |\leftrightarrow\rangle)$ , again with zero overlap. In every set, one state is identified with the logical bit value zero, the other with the logical bit value one.

Since  $|+\rangle$  and  $|\uparrow\rangle$  are non-orthogonal, their overlap is non-vanishing:  $\langle+|\uparrow\rangle = \frac{1}{\sqrt{2}}$ . The same non-orthogonality holds for any other combination of states from different sets. Given a state from any of the two sets, the very laws of quantum mechanics render it impossible to perfectly distinguish between the states! Planck and Bohr proceed in the quantum stage as follows.

- Planck randomly chooses a bit value, and also randomly chooses one of the two sets to encode the bit. The encoded state is sent to Bohr *without* announcing the set which is used for encoding.
- Bohr randomly chooses one of the two sets, and detects the signal in the appropriate basis.

After a number of bits have been transmitted this way, Planck and Bohr announce which encoding/measurement bases they have chosen. Incompatible events where different sets were utilised are ignored, and only compatible events are kept for further processing. This is commonly referred to as *sifting*. Assuming perfect hardware, Bohr's measured results should completely agree with the states sent by Planck, and they can easily check this by announcing a small number of sent/received values. If Einstein has interacted with the signals, he will have introduced noise because of the indistinguishability of non-orthogonal quantum states. This leads to discrepancies of the bit values in the selected subset, and thus his presence can be detected. We emphasise that this is impossible in a purely classical scenario where signals can be measured without introducing additional noise.

### 3.2 SARG04

Introduced two decades later than BB84, SARG04 [5] keeps the tradition of naming QKD protocols by their inventors. The same hardware components as for BB84 are required. The whole quantum stage of SARG04 is identical to BB84. What differs, however, is how bit values are extracted from the quantum measurements. The four states available are now denoted by  $|S_0\rangle, \dots, |S_3\rangle$ , and the relation  $|S_{(n+m) \bmod 4}\rangle = R^n |S_m\rangle$  ( $R$  denotes an apt rotation) holds. Four sets  $\{R^k |S_0\rangle, R^k |S_1\rangle\}, k \in \{0, 1, 2, 3\}$  are declared.

After the quantum stage is finished, Planck does not announce his bases to Bohr, but only reveals one of the subsets that contains the state which has been sent. If Bohr's measurement outcome is orthogonal to one of the two states in the set, he can conclude that the other state in the set has been sent, and he has obtained a conclusive result. It is also possible to obtain non-conclusive results, namely if the result is not orthogonal to all states in the set. After repeating this procedure for all signals, Bohr announces where he has found conclusive and inconclusive results, and the protocol commences as for BB84.

### 3.3 Decoy state variants

The main advantage of QKD is the ability to detect eavesdroppers on the line. If imperfect and lossy components (which cannot be avoided in reality) are used to implement such systems, opportunities may

arise for Einstein which allow him to mimic the behaviour of imperfections as a hideout (we will discuss usual weaknesses of QKD systems and corresponding attacks further below). It is thus essential to test and characterise the utilised hardware not only when a setup is installed, but also during the quantum stage of a running protocol. One method to perform these tests is the decoy method. In Section 4.1, we introduce an attack which can at present only be detected by these means.

### 3.3.1 Active decoy state selection

Decoy states are an extension to p&m QKD protocols. In addition to the transmitted quantum states used for signal generation, Planck actively inserts another set of states – called *decoy states* [6, 25, 39–45] – at random times. It is essential that the decoy states have slightly different intensities than the signals, but are indistinguishable from the proper signals in any other property. Since Einstein cannot distinguish between signal and decoy states, he will perform the same attacks on both, but owing to the slightly different intensities, the attack has varying effects on signals and decoys.

Following the quantum stage, Planck announces the position of the decoys in the signal stream, and Bohr announces his measurement results. By comparing the error rates for signal and decoy states, Planck and Bohr can infer photon-number resolved characteristics of the channel without using photon-number sensitive hardware. This yields very good estimates which are required for security proofs.

### 3.3.2 Passive decoy state selection

It is crucial that signal and decoy states are experimentally indistinguishable. In a laser-based implementation, the exact intensity can be difficult to control if it is varied for different signals. Great care is required to ensure that intensity modifications do not inadvertently modify other, unrelated parameters. However, it is possible to perform the generation of decoy states in the classical stage *after* the quantum transmission is finished, thus rendering a distinction between signal and decoy impossible *in principle*. The setup required for this is depicted on the left hand side of Fig. 3.

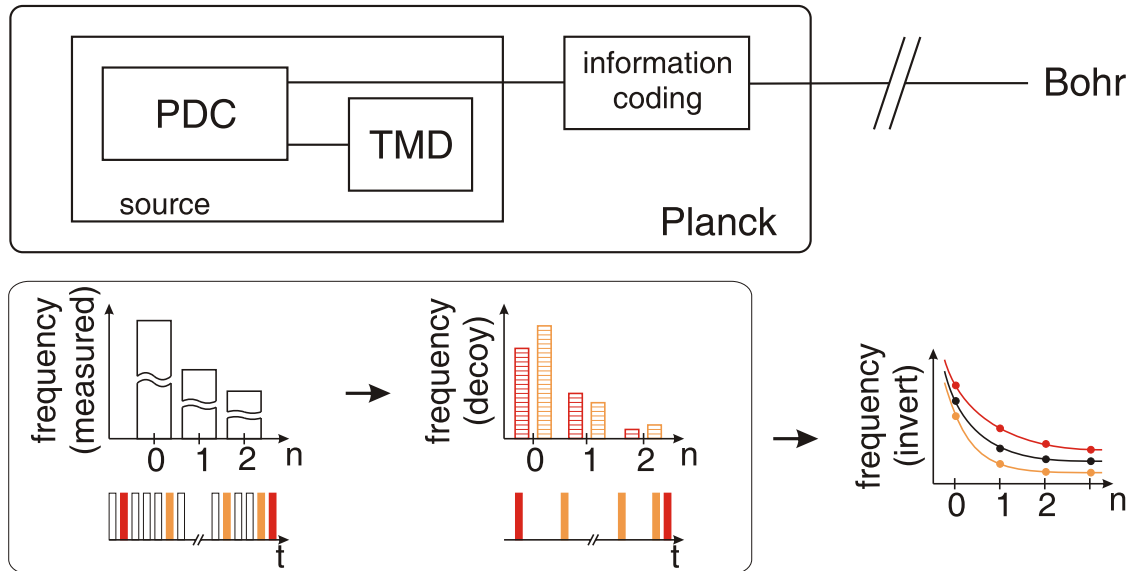


**Fig. 3** Schematic implementation of the passive decoy QKD scheme (top), and how passive decoy state selection is performed (bottom). Refer to the text for further information.

A PDC source on Planck's side generates two output states with strict photon number correlations from an incident laser pulse. The time multiplexing (i.e., approximately photon number resolving) [46, 47]



detector (TMD) in one output arm is used to trigger on the spontaneous emission of PDC photons and also to choose decoy states in the signal arm. Information encoding is performed on the signal arm, and afterwards, the state is sent to Bohr via a quantum channel and analysed there as usual.

While photon number resolution cannot be obtained for single signals, it becomes very reliable for a large number of measurements. An inversion process can transform the measured statistics into the real, sent statistics [48]. This allows to select decoy states *after* the quantum stage [25]. Even Planck and Bohr do not know which states are decoys and which states are signals during transmission. Thus it is impossible *in principle* for Einstein to distinguish between signal and decoy states. The state selection is demonstrated on Fig. 3.

The TMD records the measured photon number for each signal such that a measured statistics can be obtained. The connection between sent statistics  $\vec{p} = (p_0, p_1, \dots, p_N)$  and measured statistics  $\vec{q}$  is given by  $\vec{q} = \mathbf{C} \cdot \mathbf{L} \cdot \vec{p}$ , where  $\mathbf{L}$  is a matrix which compensates for lossy detection and  $\mathbf{C}$  accounts for convolution effects in the detector. See Ref. [47] for more details.

This inversion process is not only possible for the whole set of transmitted states, but also for (sufficiently large) subsets. To generate decoys, a measured subset with a slightly different probability distribution as the global set is selected. Inversion leads to a slightly different real statistics than for the global set. The states in the selected subset are then interpreted as decoys.

### 3.4 Entanglement based schemes

PDC sources also allow to implement entanglement based QKD schemes. While the states generated by PDC sources are always photon number correlated, it is also possible to include other degrees of entanglement, e.g., in frequency or in polarisation [49, 50]. In Ref. [37], a QKD scheme based on entangled PDC states was introduced. The state emitted from the source has the form

$$|\psi\rangle \propto \sum_{n=0}^{\infty} p(n) \sum_{m=0}^n (-1)^m |(n-m) \uparrow, m \leftrightarrow\rangle |m \downarrow, (n-m) \leftrightarrow\rangle. \quad (5)$$

For instance,  $n = 1$  delivers the Bell state  $|\psi_1\rangle \propto |\uparrow\downarrow\rangle |\leftrightarrow\rangle - |\leftrightarrow\rangle |\uparrow\downarrow\rangle$ . A crucial point is that the source needs not be placed on Planck's side, but can also reside in the middle between Planck and Bohr. While this may sound insecure at a first glance, it is indeed possible to show that this method is completely secure if Planck and Bohr can proof the entanglement of the state [51].

Although entanglement based systems tend to provide a better theoretical performance than p&m implementations, their physical realisation can be challenging, cf. p. 176 in [8].

## 4 Security proofs

The basics of QKD protocols are easy to understand, but proving unconditional security has shown to be very hard when imperfections are included. The first proof by Mayers [52], for instance, required 56 pages filled with calculations! Nowadays, proofs which employ rather different techniques are available. We should like to emphasise two particular methods.

- Information-theoretic techniques (ITT), most notably developed in [9], provide mathematically sophisticated methods to prove the security of QKD under very general assumptions. However, involved methods [10] are required to compute actual numerical values for key rates and alike.
- The security proof by Gottesman, Lo, Lütkenhaus, and Preskill (GLLP, [53]) might be less elegant than the aforementioned method, but facilitates easy calculation of actual performance data.

Results and performance achieved by GLLP-type methods are approximately identical with ITT results, and have a more direct and accessible physical interpretation. We will therefore concentrate on these in the following. Note, that all proofs rely on the law of large numbers. This requires transmission of a

nearly infinite number of pulses. For obvious reasons, this is hard to achieve in practice. The key rates for comparably small numbers of transmitted signals ( $\approx 10^4$ ) will thus decrease in comparison to the numbers presented here, cf. [54] for a detailed analysis.

#### 4.1 Possible attacks

Owing to the historical development of security proofs, three different types of attacks are conventionally distinguished.

- *Individual attacks* restrict Einstein to attaching an independent probe system to one signal after another, and measuring these probes also one after another.
- *Collective attacks* similarly restrict Einstein to attaching an independent probe to each pulse, but allow him to measure several probes collectively.
- *Coherent attacks* are the most general form where Einstein can process an arbitrary number of qbits at one time.

We mention that all rate formulae used in the remainder of this paper hold against coherent attacks.

One particular example for an individual attack often employed in proofs is an intercept-resend attack. Einstein measures each signal coming from Planck. He stores the result, and prepares a fresh pulse with his measurement result which is sent to Bohr. Assuming the BB84 protocol, only 50% of his bases choices will be compatible with the signal. These measurements lead to the correct result. The remaining 50% of the results will be random. Bohr finds that 25% of all signals are erroneous. This is no problem if the hardware induces an error rate below 25%. The protocol is aborted if this threshold is exceeded. If the errors caused by the hardware alone are above 25% percent, Planck and Bohr will not be able to detect an intercept-resend attack, and security cannot be guaranteed any more. The upper bound on the distance shown in Fig. 1 actually arises due to the intercept-resend attack. It should however be noted that this is not the smallest upper bound, cf., for instance, Ref. [12, 13] on how to compute smaller bounds.

One particularly powerful attack in p&m schemes is photon number splitting [55]. After replacing the lossy quantum channel by a loss-less one, Einstein performs a non-destructive measurement of the photon number and then adapts her action accordingly. He blocks all single photon pulses. For multi-photon pulses, he strips off one photon, stores it, and sends the remaining ones to Bohr. After Planck has announced his encoding bases, Einstein measures the stored photons and obtains full information. This strategy does not increase the error rate at all if the photon number distribution sent by Einstein is identical to the distribution which would have been expected after transmission through a lossy channel. In fact, the attack can only be detected in p&m schemes if the decoy method is employed.

#### 4.2 Anatomy of GLLP-style proofs

We now discuss the results of the GLLP security proof in order to apply it to practical QKD setups to estimate the performance of such systems. Without going into details of the derivation (which can be found in [53]), we analyse the contributions to the rate equation. An adaption of the GLLP lower bound on the secret key rate to BB84 with decoy states and one-way communication as derived by Lo and coworkers [39] in 2005 is given by

$$S_{\text{one-way}} \geq \underbrace{qQ_{\bar{N}}}_{\text{Conclusive signals}} \left( \underbrace{-f(E_{\bar{N}})H_2(E_{\bar{N}})}_{\text{Error correction}} + \underbrace{\Omega \cdot (1 - H_2(e_1))}_{\text{Privacy amplification}} \right). \quad (6)$$

Note that the value of  $S$  denotes the key generation rate, i.e., the fraction of secret bits which can be extracted per signal. The bit rate per second can be obtained by multiplying  $S$  with the repetition rate of the scheme.  $\bar{N}$  specifies the mean photon number of the source in use.  $E_{\bar{N}}$  is the overall bit error rate,

and  $e_n$  the photon number resolved bit error rate. We emphasise that the formula holds for sources with arbitrary photon number distributions.

First of all, secret bits can only be extracted from events where Bohr has obtained a conclusive result. Cases where signals are lost in the channel are excluded by the prefactor  $Q_{\bar{N}}$ . This factor denotes the fraction between successful detection events on Bohr's side and the number of pulses sent by Planck. The rate of conclusive single-photon events over all conclusive events is given by  $\Omega = \frac{Q_1}{Q_{\bar{N}}}$ . Since the detection bases need to be identical to obtain a conclusive result, the sifting factor  $q$  specifies the probability that Planck and Bohr choose identical bases. The sifting stage is not necessary, though, if a very large number of signals are transmitted, cf. [56]. This also holds for any other p&m protocol considered in the following. Two operations need to be performed on the raw bits (a visual summary of these operations can be found in Fig. 2).

- Error correction ensures that Planck and Bohr share a completely correlated string of zeroes and ones. This can be achieved by classical error correction algorithms (cf. Ref. [7, 8]). A certain number of bits needs to be sacrificed to perform the correction. The Shannon entropy  $H_2(E_{\bar{N}})$  quantifies how many. Since the Shannon limit is not constructive, practical codes will perform less efficient. This is accounted for by a compensation factor  $f(E_{\bar{N}})$ ,  $f \geq 1$ .
- Although Planck and Bohr share an identical key after error correction, Einstein may still be correlated with the key. To remove these correlations, privacy amplification [7, 8] is employed. Since only single photon signals are secure,  $\Omega$  is the base quantity for privacy amplification. Additionally, only error-free single photons can contribute, which is accounted for by the factor  $1 - H_2(e_1)$ .

While error correction can be performed equally efficient irregardless of one- or two-way communication, PA is more powerful if Planck and Bohr can perform bidirectional classical communication. The rate equation which includes two-way communication is as follows [57, 58].

$$S_{\text{two-way}} \geq q\tilde{r}_B Q_{\bar{N}} \left( -f(\tilde{E}_{\bar{N}})H_2(\tilde{E}_{\bar{N}}) + \tilde{\Omega} \cdot (1 - H_2(\tilde{e}_{1,p})) \right). \quad (7)$$

Eq. 7 is structurally similar to Eq. 6, but differs in some details. First of all, bidirectional PA works in steps on the classical bit string. In each step, roughly half of the total bits survive, but Einstein has less information on the shortened bit string. After  $n$  PA steps,  $r_B \approx 2^{-n}$ . Additionally, symmetry between bit ( $e_{n,b}$ ) and phase ( $e_{n,p}$ ) error rates is lost. Bidirectional PA reduces the overall error rates  $E_{\bar{N}}$  as well as  $\Omega$ , and makes the combination  $e_{n,b}$  and  $e_{n,p}$  more favourable. Quantities with a tilde represent the new values after performing the PA steps. We do not want to list the transformation equations, but refer the reader to Ref. [58].

### 4.3 Koashi-Preskill proof for entangled states

The key generation rate formula for the entanglement-based PDC QKD as introduced in Section 3.4 is not based on the GLLP proof. Instead, Ma and co-authors [37] founded their proof on a technique introduced by Koashi and Preskill [59]. The resulting formula is as follows

$$S \geq q(Q_{\bar{N}}[1 - f(E_{\bar{N}})H_2(E_{\bar{N}}) - H_2(E_{\bar{N}})]). \quad (8)$$

Again, the structure is similar to Eq. (6) and (7), with one important difference. The error rates need not be known for single photons, it suffices to know the overall error rate. Intuitively, one reason for this is that entanglement-based schemes are not affected by photon-number splitting operations, cf. Ref. [8].

## 5 Performance analysis

Having introduced various protocols and how experimental imperfections are included in their security proofs, we now discuss how these imperfections influence the performance quantitatively. We will compare

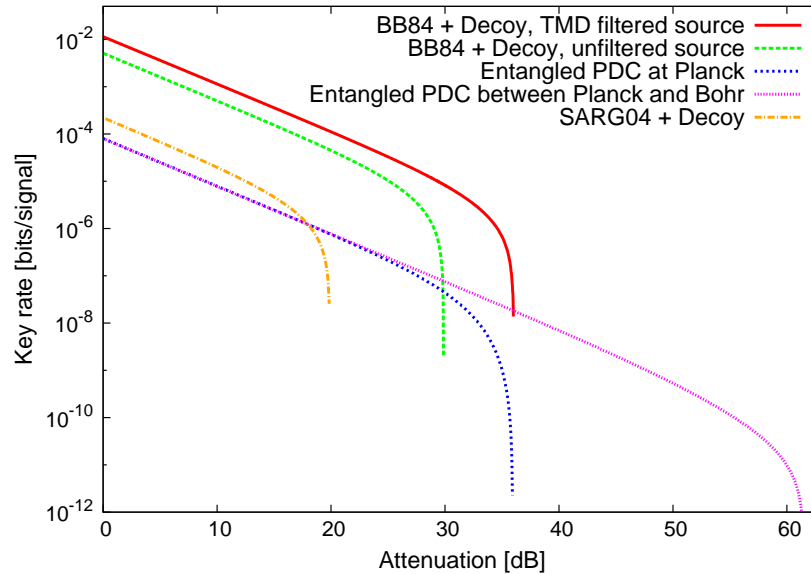


**Fig. 4** Comparison between various QKD protocols. The plot depicts lower bounds on the secret key rates.

the benefits which arise when the individual components of a QKD system are improved. This will aid experimental researchers in finding where physical and technical improvements will pay off most.

### 5.1 Numerical methods

To facilitate systematic comparison of various QKD schemes, we have developed a universal simulation tool which performs the necessary numerical computations. Care was taken to ensure that no special knowledge about security proofs or the numerics associated with them is necessary. A graphical user interface enables to conveniently obtain all data of interest. The tool will be made available for download on our group's web page<sup>4</sup>.

### 5.2 Comparison between protocols

First of all, it is desirable to know how the protocols perform compared to each other when the same hardware is employed. Fig. 4 provides a series of performance plots for all protocols discussed in this paper. All use the hardware described in the GYS experiment [60].

The largest distance is achieved by the entangled PDC protocol, which exceeds the tolerable loss of other protocols by more than 25 dB. The achievable key rate, however, is two orders of magnitude lower than for BB84 decoy protocols with and without source filtering. It can also be argued that entanglement based protocols are harder to implement than p&m protocols, cf. [8].

Using SARG04 instead of BB84 does not provide any advantages when the security proofs utilised in this paper are employed.<sup>5</sup> Both, secret key rate and secure distance are smaller than for BB84 with decoy states. For these reasons, we focus on the BB84 decoy protocol in the following.

<sup>4</sup> <http://www.optik.uni-erlangen.de> → Max Planck Junior Group IQO → Quantum Cryptography.

<sup>5</sup> Note, however that this can change when different security analyses are employed. With the methods introduced in Ref. [5], SARG performs better than BB84, but the analysis does not employ decoy states.

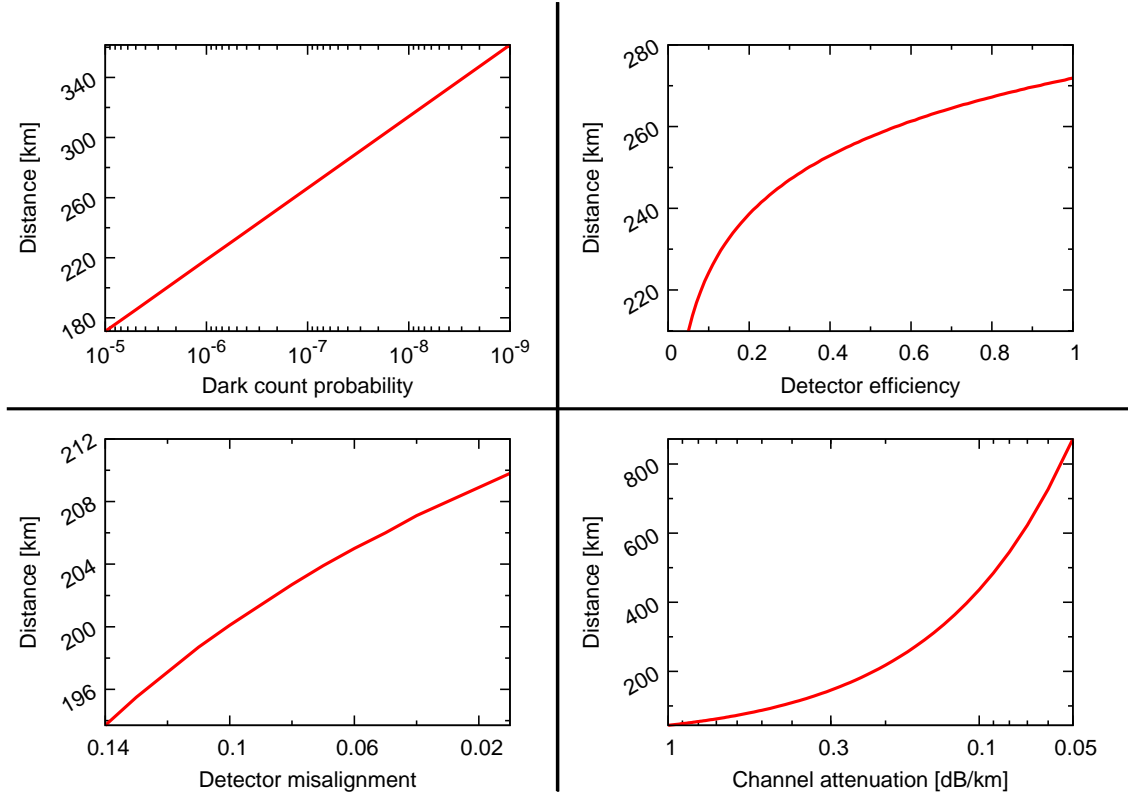


**Fig. 5** Comparison of achievable secure distances when experimental imperfections are varied. The standard parameters are  $p_{\text{dark}} = 1.7 \cdot 10^{-6}$ ,  $\alpha = 0.21$  dB/km,  $e_{\text{det}} = 3.3 \cdot 10^{-2}$ ,  $q = 1$ ,  $\lambda = 1550$  nm,  $\eta_{\text{det}} = 4.5 \cdot 10^{-2}$ , and the protocol is decoy based BB84. Refer to the text for further information.

### 5.3 Quantitative influence of imperfections

Before we discuss any specific scenarios, we would like to present a general summary how the achievable secure distance changes with experimental imperfections. The corresponding graphs can be found in Fig. 5.

Little improvement can be expected when the detector misalignment is improved. The current experimental standard is  $e_{\text{det}} = 0.03$ . If this value were reduced to 0.02, the increase in secure distance is only around 3 km. Even a very large misalignment of 10% causes only approximately 8 km decrease.<sup>6</sup> This also implies that slightly different efficiencies or dark count rates of the two detectors can be mostly neglected.

Improving channel attenuation would be highly beneficial as the bottom right graph in Fig. 5 demonstrates. However, the damping for telecommunication fibres is quite close to the optimal technological possibilities as we have explained before. Bad weather drastically increases free space damping and thus shortens the secure distance considerably. Furthermore, the constantly varying conditions need to be monitored during signal transmission.

Moderate possibilities for improvement are provided by optimised detection efficiency. Observe the top right graph in Fig. 5. Improving  $\eta_{\text{det}}$  from, say, 10% to 60% results in a increased secure distance of approximately 30 km.

We find that the best possibility to increase the secure distance is to suppress dark counts, as can be seen in the top left side of Fig. 5. Decreasing this rate by one order of magnitude delivers 40 additional secure kilometres. Considering the development over the last years, it is realistic to assume that better time gating

<sup>6</sup> Note, that for simplicity we neglect weakly basis dependent attacks [53] here.

Ref.	Protocol	$\lambda$ [nm]	Mean photon #	$\alpha$	$\eta_{\text{det}}$	$\epsilon_{\text{det}}$	$p_{\text{dark}}$	Enc.	QBER
[61]	BB84 + Decoy	1550	signal: 0.55 decoy: vac., 0.098	unspec.	5.62%	unspec.	$1.4 \cdot 10^{-4}$	Pol.	unspec.
[60]	BB84	1550	0.0042 – 0.046	0.21 dB/km	4.5%	3%	$8 \cdot 10^{-7}$	Phase	3 – 6%
[62]	BB84 + Decoy	1550	signal: 0.6 decoy: vac., 0.2	0.2 dB/km	unspec.	unspec.	$6.7 \cdot 10^{-6}$ – $9.2 \cdot 10^{-6}$	Pol.	3.2% – 3.6%
[63]	BB84 + Decoy	1550	signal: 0.6 decoy: 0.2	unspec.	unspec.	unspec.	$5 \cdot 10^{-7}$	Phase	1 – 2%
[64]	BB84 + Decoy	1550	signal: 0.425 decoy: 0.204	4.7 dB/ 25.3 km	5.6%	unspec.	$9.4 \cdot 10^{-5}$	Pol.	1.72%
[65]	Entangled	810	unspec.	1.4%/ 7.8 km	15%	unspec.	$800 \text{ s}^{-1}$	Pol.	9.9%
[66]	BB84 + Decoy	850	signal: 0.27 decoy: vac., 0.39	24 dB/ 144 km	10%	3%	unspec.	Pol.	6.48%

**Table 1** Summary of parameters used in recent QKD experiments.

and new detectors with increased single photon sensitivity will allow to improve  $p_{\text{dark}}$  by approximately three orders of magnitude.

## 6 Example scenarios

Let us finally turn our attention to four practical scenarios. We base our analysis on a number of QKD experiments performed in recent years. The parameters of components employed for them is collected in Table 1.

### 6.1 Radio link free space transmission

Short distance QKD between buildings in a city, for instance, can conveniently be realised via radio links operating at 800 nm. Because of stray light at daytime, such schemes will only be operational at night. Another crucial factor is signal attenuation. Weather conditions impose serious differences in loss per length. This in turn has a considerable effect on the achievable key generation rate. Fig. 6 shows the performance for a wide range of attenuation values. While the key rate at best conditions gives values in the satisfactory range of  $10^{-3}$  bits per pulse, performance will rapidly decrease with increasing attenuation. In bad weather, the channel loss can be in the range of  $20 \frac{\text{dB}}{\text{km}}$ , and the secure distance will only be around 10 km, which is often not sufficient for any communication at all.

### 6.2 Satellite-based QKD

Recently, experimental free space QKD implementations [66] have reached transmission distances which would allow to communicate with geostationary satellites.<sup>7</sup> This is an important break-through because it would enable a world-spanning secure QKD network. Since transmission losses from the earth into space cannot be actively influenced, the detector efficiency is the main parameter which can be improved. The implementation from op. cit. employed a detector with a quantum efficiency of 10%. Fig. 7 shows how the secure key rate would develop with better detection efficiency (clearly, the absolute value of the maximal transmission distance is not of interest because the path length from a ground station to the satellite is fixed). While the quoted detection efficiency barely suffices to reach the desired distance, a increase by 20 to 30 absolute percent would move the rapidly declining part of the key rate to distances beyond the satellite. The desired transmission distance now lies in the slowly falling part, resulting in a secret key rate increased by many orders of magnitude.

<sup>7</sup> The attenuation between earth and a geostationary satellite is around 35 dB.

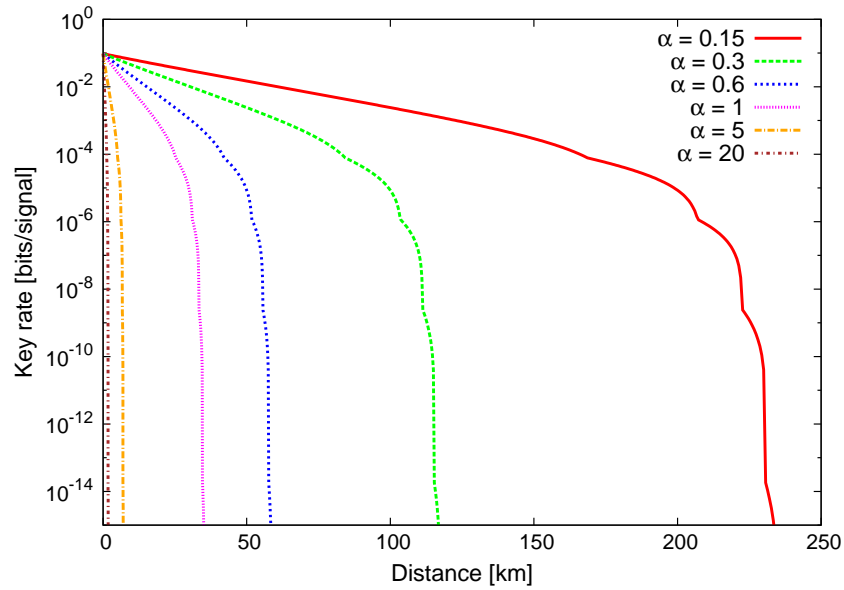


**Fig. 6** Performance analysis for radio link based QKD systems. The plot depicts lower bounds on the secret key rates. Refer to the text for more information. The connection between attenuation per length  $\alpha$ , channel length  $L$ , and loss  $\eta$  is given by  $\eta = 10^{-\alpha L/10}$ .

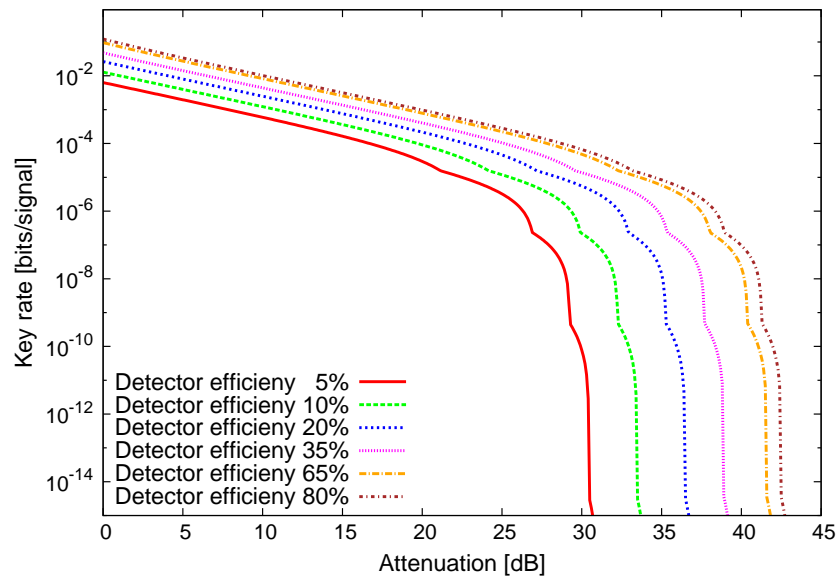


**Fig. 7** Influence of detector efficiency for a satellite link on the secure key generation rate.

### 6.3 Long-Distance fibre based transmission

The most promising candidate for intermediate to long range terrestrial communication are fibre-based systems operating at 1550nm. Several experiments in this regime have been performed recently [60–64]. The key parameter which provides room for improvement is the dark count probability. While the detectors in the quoted papers provide probabilities in the range between  $10^{-5}$  and  $10^{-6}$ , it can reasonably be

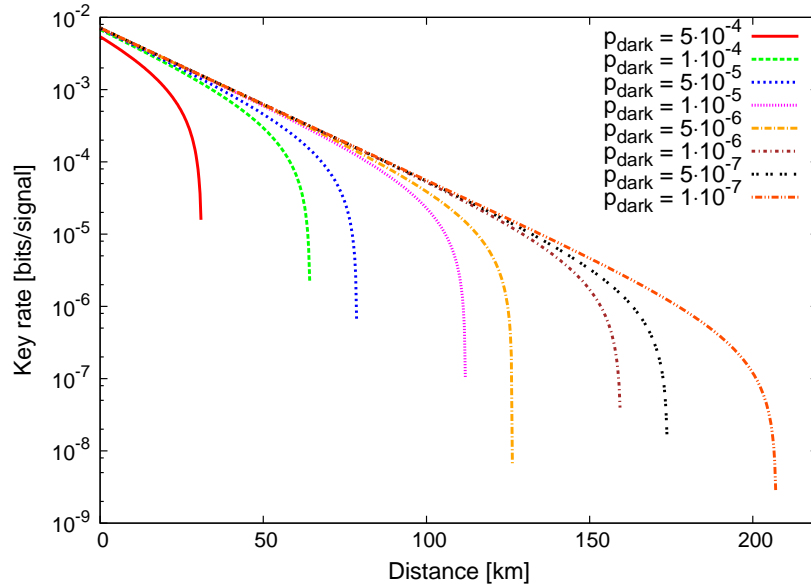


**Fig. 8** Influence of detector efficiency in a fibre based system at 1550 nm on the secure key generation rate.

expected that the probability will be as low as  $10^{-9}$  in future detectors. Fig. 8 demonstrates that while the rates are unaffected by the dark count rates, the secure distance increases considerably with decreasing dark count probability.

#### 6.4 Passive decoy QKD with two-frequency downconversion

Transmission over fibres is advantageous for wavelengths in the 1550nm regime, but good detectors are only available for 800nm. Particular advantages gained by employing one wavelength region are always negated to some extent in conventional QKD setups. A proposed setup is a variation of the scheme introduced in Section 3.3.2. It tries to overcome this limitation by picking advantageous features from both worlds. As long as energy and momentum are conserved via (quasi)-phase-matching, downconversion sources can well be built to emit signal and idler photons at different wavelengths. Signals are emitted at 1550 nm and transmitted over a quantum channel with little loss. The idler arm emits photons at 800 nm; these can be detected by the TMD with good quantum efficiency (around 70%). Fig. 9 presents the performance prediction for the proposed scheme. The graph is based on a source repetition rate of 20 MHz, Ref. [14] has shown that this is the maximum for TMD detection with current technology. While the maximal secure distance is identical in both cases, the mixed wavelength scheme provides a bit transmission rate which is one order of magnitude higher than for identical wavelengths.

## 7 Conclusions

In summary, we have presented a selection of discrete variable quantum key distribution systems. After analysing the structure of the rate formulae obtained from security proofs, we have given a systematic comparison of experimental tunables and their influence on the performance. The areas where experimental improvements will bring maximal benefit have been exposed. Finally, we have performed an analysis of four practical scenarios under consideration of current experimental possibilities.

**Acknowledgements** We would like to thank Benjamin Brecht for his most valuable and long-standing help with image preparation.



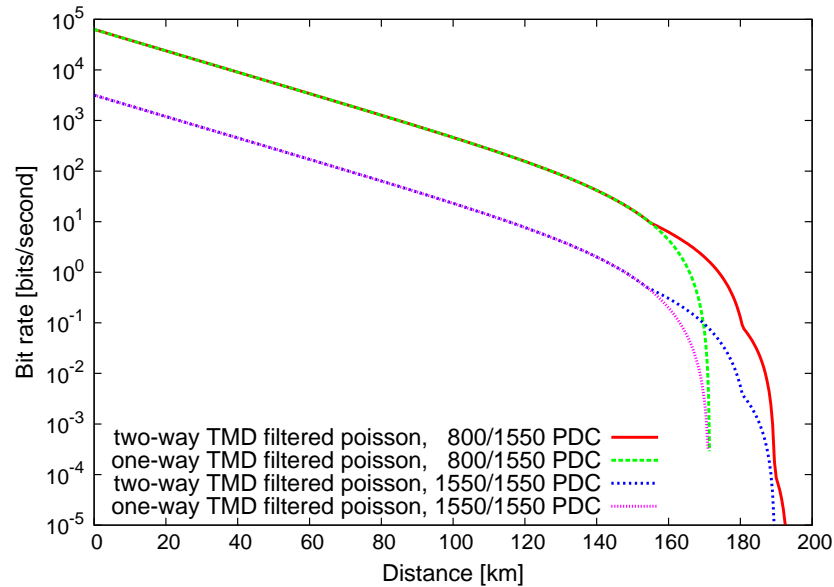


**Fig. 9** Performance prediction for a mixed-wavelength passive decoy scheme. The signals emitted at 1550 nm are transferred over a quantum channel, while the idler photons at 800 nm are used for triggering and passive decoy selection with good quantum efficiency. The secure key rate in comparison to a passive decoy scheme with signal and idler wavelengths at 1550 nm is considerably increased.

## References

- [1] S. Wiesner, *Sigact News* **15**, 1 (1983).
- [2] C. H. Bennett and G. Brassard, in: *Proc. IEEE Int. Conf. on Computers, Systems, and Signal Processing*, (IEEE, New York, 1984) pp. 175–179.
- [3] C. H. Bennett, G. Brassard, and A. K. Ekert, *Scientific American* **267**, 50–57 (1992).
- [4] A. K. Ekert, *Phys. Rev. Lett.* **67**(6), 661–663 (1991).
- [5] V. Scarani, A. Acin, G. Ribordy, and N. Gisin, *Phys. Rev. Lett.* **92**, 057901 (2004).
- [6] W. Y. Hwang, *Phys. Rev. Lett.* **91**, 057901 (2003).
- [7] M. Dušek, N. Lütkenhaus, and M. Hendrych, *Prog. in Opt.* **49**, 381 (2006).
- [8] N. Gisin, G. Ribordy, W. Tittel, and H. Zbinden, *Rev. Mod. Phys.* **74**, 145 (2002).
- [9] R. Renner, N. Gisin, and B. Kraus, *Phys. Rev. A* **72**, 012332 (2005).
- [10] B. Kraus, N. Gisin, and R. Renner, *Phys. Rev. Lett.* **95**, 080501 (2005).
- [11] C. H. F. Fung, K. Tamaki, and H. K. Lo, *Phys. Rev. A* **73**, 012337 (2006).
- [12] T. Moroder, M. Curty, and N. Lütkenhaus, *Phys. Rev. A* **73**, 012311 (2006).
- [13] T. Moroder, M. Curty, and N. Lütkenhaus, *Phys. Rev. A* **74**, 052301 (2006).
- [14] H. B. Coldenstrodt-Ronge and C. Silberhorn, *J. Phys. B* **40**(19), 3909–3921 (2007).
- [15] M. Keller, B. Lange, K. Hayasaka, W. Lange, and H. Walther, *Nature* **431**(7012), 1075–1078 (2004).
- [16] L. Mandel and E. Wolf, *Optical Coherence and Quantum Optics* (Springer, Heidelberg, 1995).
- [17] M. Avenhaus, et al., in preparation (2007).
- [18] P. R. Tapster and J. G. Rarity, *J. Mod. Opt.* **45**(3), 595–604 (1998).
- [19] O. Alibart, D. B. Ostrowsky, P. Baldi, and S. Tanzilli, *Elect. Lett.* **30**(12), 1539–1541 (2005).
- [20] A. U'Ren, C. Silberhorn, K. Banaszek, I. A. Walmsley, R. Erdmann, W. P. Grice, and M. G. Raymer, *Laser Physics* **15**, 146 (2005).
- [21] A. B. U'Ren, C. Silberhorn, K. Banaszek, and I. A. Walmsley, *Phys. Rev. Lett.* **93**, 093601 (2004).
- [22] T. Horikiri, H. Sasaki, H. Wang, and T. Kobayashi, *Phys. Rev. A* **72**(1), 012312 (2005).
- [23] T. Horikiri and T. Kobayashi, *Phys. Rev. A* **73**, 032331 (2006).
- [24] Y. Adachi, T. Yamamoto, M. Koashi, and N. Imoto, *Phys. Rev. Lett.* **99**(18), 180503 (2007).
- [25] W. Mauerer and C. Silberhorn, *Phys. Rev. A* **75**(5), 050305(R) (2007).
- [26] N. Lütkenhaus, *Phys. Rev. A* **61**, 052304 (2000).

- [27] S. Tanzilli, H. de Riedmatten, W. Tittel, H. Zbinden, P. Baldi, M. de Micheli, D. B. Ostrowsky, and N. Gisin, *Elect. Lett.* **37**(1), 26–28 (2001).
- [28] K. Banaszek, A. U'Ren, and I. A. Walmsley, *Optics Letters* **26**, 1367–1369 (2001).
- [29] A. Fedrizzi, T. Herbst, A. Poppe, T. Jennewein, and A. Zeilinger, *Opt. Exp.* **15**, 15377–15386 (2007).
- [30] C. E. Kuklewicz, F. N. C. Wong, and J. H. Shapiro, *Phys. Rev. Lett.* **97**(22), 223601 (2006).
- [31] J. Fulconis, O. Alibart, J. L. O'Brien, W. J. Wadsworth, and J. G. Rarity, *Phys. Rev. Lett.* **99**(12), 120501 (2007).
- [32] X. Li, J. Chen, P. Voss, J. Sharping, and P. Kumar, *Opt. Express* **12**(16), 3737–3744 (2004).
- [33] J. Fulconis, O. Alibart, W. Wadsworth, P. Russell, and J. Rarity, *Opt. Express* **13**(19), 7572–7582 (2005).
- [34] W. K. Wootters and W. H. Zurek, *Nature* **299**(5886), 802–803 (1982).
- [35] G. S. Vernam, *J. AIEE* **45**(109) (1926).
- [36] S. L. Braunstein and P. van Loock, *Rev. Mod. Phys.* **77**(2), 513–577 (2005).
- [37] X. Ma, C. H. F. Fung, and H. K. Lo, *Phys. Rev. A* **76**(1), 012307 (2007).
- [38] P. W. Shor and J. Preskill, *Phys. Rev. Lett.* **85**, 000441 (2000).
- [39] H. K. Lo, *J. Quant. Inf.* **3**, 143–143 (2005).
- [40] J. B. Li and X. M. Fang, *Chinese Phys. Lett.* **23**(4), 775–778 (2006).
- [41] X. F. Ma, B. Qi, Y. Zhao, and H. K. Lo, *Phys. Rev. A* **72**(1), 012326 (2005).
- [42] X. B. Wang, C. Z. Peng, and J. W. Pan, *Appl. Phys. Lett.* **90**, 031110 (2007).
- [43] X. B. Wang, *Phys. Rev. A* **75**(5), 052301 (2007).
- [44] X. B. Wang, *Phys. Rev. A* **72**(1), 012322 (2005).
- [45] X. B. Wang, *Phys. Rev. Lett.* **94**, 230503 (2005).
- [46] M. J. Fitch, B. C. Jacobs, T. B. Pittman, and J. D. Franson, *Phys. Rev. A* **68**, 043814 (2003).
- [47] D. Achilles, C. Silberhorn, C. Sliwa, K. Banaszek, I. A. Walmsley, M. J. Fitch, B. C. Jacobs, T. B. Pittman, and J. D. Franson, *J. Mod. Opt.* **51**(9-10), 1499–1515 (2004).
- [48] D. Achilles, C. Silberhorn, and I. A. Walmsley, *Phys. Rev. Lett.* **97**, 043602 (2006).
- [49] C. Kurtsiefer, M. Oberparleiter, and H. Weinfurter, *Phys. Rev. A* **64**, 023802 (2001).
- [50] P. G. Kwiat, K. Mattle, H. Weinfurter, A. Zeilinger, A. V. Sergienko, and Y. H. Shih, *Phys. Rev. Lett.* **75**(24), 4337–4341 (1995).
- [51] M. Curty, M. Lewenstein, and N. Lütkenhaus, *Phys. Rev. Lett.* **92**(21), 217903 (2004).
- [52] D. Mayers, *Journal of the ACM* **3**, 35 (1998).
- [53] D. Gottesman, H. K. Lo, N. Lütkenhaus, and J. Preskill, *Quant. Inf. & Comp.* **4**(5), 325–360 (2004).
- [54] T. Meyer, H. Kampermann, M. Kleinmann, and D. Bruß, *Phys. Rev. A* **74**, 042340 (2006).
- [55] N. Lütkenhaus and M. Jahma, *New Journal of Physics* **4**, 44.1–44.9 (2002).
- [56] H. K. Lo, H. F. Chau, and M. Ardehali, *Journal Of Cryptology* **18**(2), 133–165 (2005).
- [57] D. Gottesman and H. K. Lo, *IEEE Transactions on Information Theory* **49**(2), 457–475 (2003).
- [58] X. Ma, C. H. F. Fung, F. Dupuis, K. Chen, K. Tamaki, and H. K. Lo, *Phys. Rev. A* **74**, 032330 (2006).
- [59] M. Koashi and J. Preskill, *Phys. Rev. Lett.* **90**(5), 057902 (2003).
- [60] D. Gobby, Z. Yuan, and A. Shields, *Appl. Phys. Lett.* **84**, 19 (2004).
- [61] J. F. Dynes, Z. L. Yuan, A. W. Sharpe, and A. J. Shields, *Opt. Exp.* **15**, 8465 (2007).
- [62] C. Z. Peng, J. Zhang, D. Yang, W. B. Gao, H. X. Ma, H. Yin, H. P. Zeng, T. Yang, X. B. Wang, and J. W. Pan, *Phys. Rev. Lett.* **98**(1), 010505 (2007).
- [63] Z. Q. Yin, Z. F. Han, W. Chen, F. X. Xu, Q. L. Wu, and G. C. Guo, [arXiv.org:quant-ph/0704.2941](https://arxiv.org/abs/quant-ph/0704.2941) (2007).
- [64] Z. L. Yuan, A. W. Sharpe, and A. J. Shields, *Appl. Phys. Lett.* **90**(1), 011118 (2007).
- [65] K. Resch, M. Lindenthal, B. Blauensteiner, H. Böhm, A. Fedrizzi, C. Kurtsiefer, A. Poppe, T. Schmitt-Manderbach, M. Taraba, R. Ursin, P. Walther, H. Weier, H. Weinfurter, and A. Zeilinger, *Opt. Express* **13**(1), 202–209 (2005).
- [66] T. Schmitt-Manderbach, H. Weier, M. Fürst, R. Ursin, F. Tiefenbacher, T. Scheidl, J. Perdignes, Z. Sodnik, C. Kurtsiefer, J. G. Rarity, A. Zeilinger, and H. Weinfurter, *Phys. Rev. Lett.* **98**(1), 010504 (2007).